

## Indications of electron emission from the deuteron-deuteron threshold resonance

K. Czernski <sup>1,\*</sup>, R. Dubey <sup>1</sup>, M. Kaczmarski <sup>1</sup>, A. Kowalska <sup>2</sup>, N. Targosz-Ślęczka <sup>1</sup>, G. Das Haridas <sup>1</sup> and M. Valat <sup>1</sup>

<sup>1</sup>*Institute of Physics, University of Szczecin, 70-451 Szczecin, Poland*

<sup>2</sup>*Physics Department, Maritime University of Szczecin, 70-500 Szczecin, Poland*



(Received 5 June 2022; revised 26 November 2023; accepted 22 January 2024; published 12 February 2024)

Electron emission in the deuteron-deuteron reaction supporting existence of the single-particle threshold resonance in  $^4\text{He}$  has been observed for the first time. The measured electron energy spectrum and the electron-proton branching ratio agree very well with the assumed electron-positron pair creation decay of the  $0^+$  resonance state to the ground state and the detailed Monte Carlo simulations of the experimental energy spectrum.

DOI: [10.1103/PhysRevC.109.L021601](https://doi.org/10.1103/PhysRevC.109.L021601)

**Introduction.** The  $^4\text{He}$  level structure at excitation energies below 30 MeV seems to be very well known for the last decades and could be successfully applied for description of nuclear reaction by means of the multichannel  $R$ -matrix parametrization [1]. Recent *ab initio* structure calculations of the four-nucleon system applying realistic nucleon-nucleon interactions and the microscopic cluster approach [2–4] confirmed the known level structure of  $^4\text{He}$ , as well. Therefore, it was very surprising that the last precise measurements of the  $^2\text{H}(d, p)^3\text{H}$  reaction cross section performed on the deuterated Zr target at deuteron energies down to 5 keV [5] pointed to a strong contribution of a  $0^+$  resonance placed close to the DD reaction threshold. This new state is supposed to be a single-particle resonance having the 2+2 cluster structure, which results in a very small and energy dependent resonance width. From the theoretical point of view [5,6], the existence of the  $0^+$  threshold resonance arises from a weak coupling between the states of the 1+3 and 2+2 clustering (see Fig. 1). Whereas the  $s$ - and  $p$ -wave resonances below and close to the DD threshold at the excitation energy of about 24 MeV have almost the pure 1+3 structure, the known negative parity levels ( $0^-$ ,  $1^-$ ,  $2^-$ ) at the excitation energy of about 28 MeV show predominantly the 2+2 clustering of the relative angular momentum  $L = 1$ . Thus, in analogy to the first excited state of  $^4\text{He}$  with  $J^\pi = 0^+$  that can be interpreted as the  $s$ -wave resonance of the 1+3 cluster [7], a similar  $s$ -wave state should be also expected for the 2+2 cluster nearby the DD threshold [6].

According to the theoretical calculations based on the  $E0$  energy weighted sum rule [6] the DD threshold resonance should have a large partial width for the electron-positron pair creation and therefore, the detection of emitted electrons

with a continuous energy spectrum up to 23 MeV in the DD reactions could provide an additional argument for the existence of the threshold resonance. The latter would be of large importance for nuclear reaction rates of astrophysical plasmas and commercial applications of the DD fusion reactions. The contribution of the  $e^+e^-$  channel to the DD reaction cross section should increase for decreasing deuteron energies far below a Coulomb barrier of about 350 keV, where the DD reactions are also enhanced by the electron screening effect. The charges of reacting nuclei are shielded by surrounding electrons of the medium leading to reduction of the Coulomb barrier height and an increase of the penetration factor through the barrier. This effect is especially important for the dense stellar plasma of giant planets, brown and white dwarfs [8], where the reaction rates can increase by many orders of magnitude [9]. Investigation of the low-energy nuclear reactions in metallic environments with their quasifree electrons provides a unique occasion to compare experimental results with theoretical predictions. Many experiments carried out in the past showed large discrepancies for the screening energy values obtained for both metallic [10] and gaseous [11] targets. Thus, a precise determination of the threshold resonance parameters could help us to understand the nature of the observed enhancement of the DD reaction cross section in the energy region, where the electron screening as well as excitation of the threshold resonance take place [5].

In this Letter, we report the first indication of the electron emission in the low-energy DD reactions which can originate from the internal pair creation decay of the threshold resonance. The experimental results will be compared to the theoretical calculations of the reaction branching ratio, showing that the  $e^+e^-$  transition to the ground state of  $^4\text{He}$  should be the strongest reaction channel at very low deuteron energies. The experimental analysis will be also supported by careful Monte Carlo simulations using the GEANT4 code [12].

**Experimental setup.** The experiment was performed at the eLBRUS Ultra High Vacuum Accelerator Facility of the Szczecin University in Szczecin, Poland [13]. A deuterium beam was accelerated to energies ranging 6–16 keV, with the constant current beam of 40  $\mu\text{A}$ , using the magnetically

\*konrad.czernski@usz.edu.pl

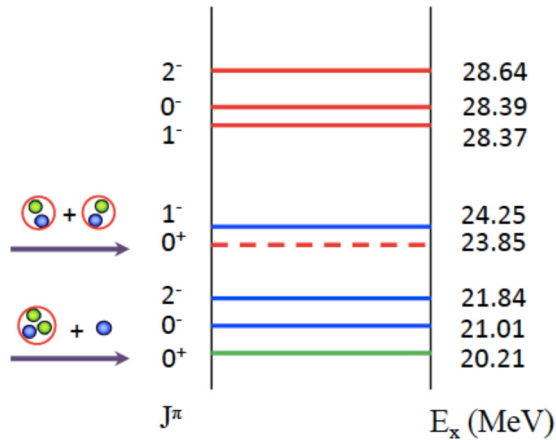


FIG. 1. Schematic energy levels of  ${}^4\text{He}$  representing  $s$ - and  $p$ -wave resonances for the 1+3 (blue) and 2+2 (red) cluster states. The arrows show the corresponding thresholds which are close to the  $0^+$  resonances. The DD threshold resonance is marked with the red dashed line.

analyzed single-charged atomic and molecular deuterium ions. The beam was impinged on a 0.5-mm-thick  $\text{ZrD}_2$  target that was tilted at  $45^\circ$  to the beam, resulting in the beam spot size of  $7 \times 12$  mm. To reduce the systematic uncertainties, only one EG ORTEC silicon detector of the 1 mm thickness and  $100\text{ mm}^2$  detection area, situated at the backward angle  $135^\circ$ , was used for all charged particles emitted: protons, tritons, and  ${}^3\text{He}$  particles as well as electrons and positrons produced by the DD reactions. Utilizing a single detector enabled us to reduce its distance to the target down to 6 cm and increase its solid angle, which was necessary due to the rapidly dropping reaction cross section for lowering deuteron energies. The traditional analog NIM bin system was used to process the energy signal created in the detector, and data were acquired via the TUKAN MCA.

In the front of the detector, an Al absorption foil was placed for two different reasons. First, the detector should be protected against elastically scattered beam deuterons. Second, the foil thickness was set to  $3.7\ \mu\text{m}$  to also absorb 0.8-MeV  ${}^3\text{He}$  particles and reduce the energy of the emitted 1.02-MeV tritons below 0.6 MeV in order to detect electrons free of background up to 1 MeV, which is the highest electron energy detectable by our Si detector (see Fig. 2). Slightly below 3 MeV, a proton peak is visible together with a low-energy tail going down to 1.5 MeV resulting from the elastically scattered protons in the absorption foil.

To be sure that the continuum part of the charged particle spectrum results from electron/positron emission, we also applied the 2- and 3-mm-thick Si detectors that fully absorb electrons of maximum energy 2 and 3 MeV, respectively. Additionally, the absorption Al foil in the front of the detector was of 45 and  $36\ \mu\text{m}$  thickness, respectively, which was enough to stop emitted tritons and reduce the energy of protons to 1.8 and 2.2 MeV, but practically did not change the energy spectrum of high energy electrons/positrons. The experimental spectrum for these cases is presented in Fig. 3. A prominent bump at energies 0.75 and 1 MeV would

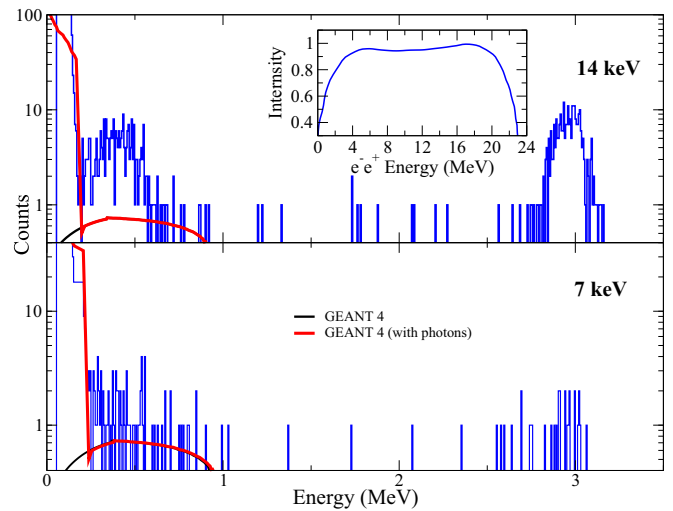


FIG. 2. Comparison between the charged particle spectra measured at two different deuteron energies and the calculated electron spectrum. Upper panel: The two distinct peaks are protons and tritons along with electrons/positrons from the DD reaction at the deuteron energy 14 keV. Bottom panel: The spectrum obtained for 7 keV. Solid lines correspond to the GEANT4 simulated spectra: electronic part only (black line) and electrons together with low energy photons (red line). The inset in the upper part presents the energy spectrum of emitted electrons/positrons from the threshold resonance according to the GEANT4 simulation. The shaded box corresponds to the electron/positron counting integration area.

correspond to the average energy loss of high energy electron/positrons in the detector (see the next section).

The energy calibration of the detector was performed with a  ${}^{241}\text{Am}$  alpha source and  ${}^{22}\text{Na}$ ,  ${}^{60}\text{Co}$ ,  ${}^{204}\text{Tl}$  beta sources with and without the Al absorption foil. In Fig. 4, the electron energy spectrum of  ${}^{204}\text{Tl}$  decaying by two different  $\beta^-$  transitions of the  $Q = 345$  and 763 keV is presented.

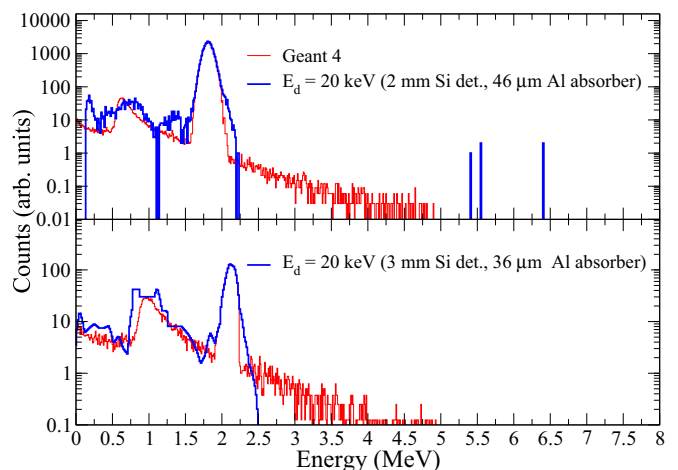


FIG. 3. Experimental energy spectrum measured at the deuteron energy 20 keV using the 2- and 3-mm-thick Si detectors with 45- and  $36\text{-}\mu\text{m}$ -thick absorption Al foils (in blue), respectively. The GEANT4 calculated spectrum is presented in red.

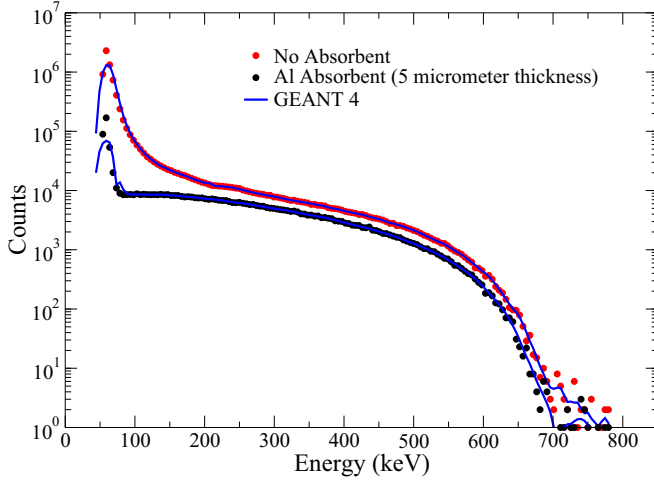


FIG. 4. Comparison between experimental and simulated energy spectra of the  $\beta^-$  radioactive source  $^{204}\text{Tl}$ . The spectra were measured with and without the 5- $\mu\text{m}$  Al absorber placed at the front of the detector.

*Simulation of the electron energy spectrum.* As explained before, we expect that the threshold resonance in  $^4\text{He}$  at the excitation energy of 23.84 MeV should decay by the internal electron-positron pair creation. To calculate the final energy spectrum of electrons registered in the Si detector, we performed a series of the Monte Carlo simulations using the GEANT4 code [12]. The computational ability can be demonstrated in Fig. 4, where the electron spectrum of the  $^{204}\text{Tl}$  radioactive source could be described very precisely. The increase of the counting rate at very low energies corresponds to the low energy photons produced due to the bremsstrahlung and secondary recombination effects, e.g., about 80-keV x rays induced in the gold surface layer of the detector (see also Figs. 2 and 3). The GEANT4 calculations were performed for different thicknesses of detectors and absorption foils and all projectile energies. The final energy spectra are the result of 100 simulation runs with  $5 \times 10^7$  electrons and  $5 \times 10^7$  photons each, leading to  $5 \times 10^9$  incident events in the detector.

The electron/positron energy spectrum calculated for the threshold resonance decay as it is expected for the thin (1 mm) detector is depicted in Fig. 2; the original energy distribution of the internal pair creation is inserted in the same figure. The maximum energy of emitted electrons amounts to 22.73 MeV, but only electrons with energy of 1 MeV or less can be fully absorbed in the detector. Therefore, the high energy electrons of the pair creation for which the detector is transparent will be registered at the energies lower than 1 MeV. The electron spectrum calculated using the GEANT4 simulations was compared to the experimental ones in Fig. 2, showing that the average energy loss of electrons/positrons in the detector is about 450 keV.

The calculated energy spectrum shows a strong increase of the counting rate for energies below 150 keV due to absorbed photons similar to the spectra measured for the  $^{204}\text{Tl}$  radioactive source. Without the photonic contributions, the energy spectrum strongly drops. The theoretical spectrum fits very

well the experimental data obtained for different projectile energies.

In the case of the thicker (2 and 3 mm) Si detectors, the experimental spectrum can also be described quite well (see Fig. 3). The 36- and 46- $\mu\text{m}$ -thick Al foils have been chosen to fully absorb tritons and  $^3\text{He}$  particles produced in the DD reactions. The 3-MeV protons, dominating the measured spectra, lost about 0.8 MeV or 1.2 in the Al foils, respectively. A broad bump at energies around 1 MeV results from high-energy electrons for which the detector is transparent and only a part of their energy can be absorbed. The average energy loss of electrons/positrons depends only on the thickness of the detector since the stopping power of electrons in the energy range 1–20 MeV is almost constant. Details of the high-energy electron measurements with Si detectors of different thicknesses are discussed in [14]. The electron absorption bump position is not affected by the Al foils but can be a little bit shifted due to instabilities of high voltage depletion depth of detectors resulting from long-term irradiations. According to the GEANT4 simulations, at energies below 0.5 MeV, an increasing spectral contribution due to elastically backscattered electrons on the target and target holder can be also observed. Additionally, at the low-energy tail of the proton line, a small contribution from the scattered protons is visible, as well (see [14]). The GEANT4 simulations also predict observation of electron counts at energies higher than the proton line. However, integrating this part of the energy spectrum results in a few counts that are not statistically significant. Thus, the experimental data are consistent with the emission of high-energy electrons.

*Theoretical analysis.* As shown previously [6], the threshold DD resonance in  $^4\text{He}$  should have a large partial width for the electron-positron pair creation. The enhancement of the reaction yield measured for the proton channel at the deuteron energies down to 6 keV [5] could be explained by both the electron screening effect and the destructive interference of the threshold resonance with the known broad resonances of  $^4\text{He}$ . Thus, determination of the electron-to-proton branching ratio could be an independent proof for existence of the DD threshold resonance. The experimentally determined values are presented in Fig. 5. Both reaction channels are studied by the same detector, therefore the error bars arise only from the statistical uncertainties.

The screened nuclear reaction cross section for the  $^2\text{H}(d, p)^3\text{H}$  reaction can be parametrized as follows [15]:

$$\begin{aligned} \sigma_{\text{scr}}(E) &= \frac{1}{\sqrt{E(E+U_e)}} S(E) \exp\left(-\sqrt{\frac{E_G}{E+U_e}}\right) \\ &= \frac{1}{\sqrt{EE_G}} P(E+U_e) S(E), \end{aligned} \quad (1)$$

where  $S(E)$  is the astrophysical  $S$  factor, and the  $s$ -wave penetration factor through the Coulomb barrier  $P(E)$  is given by

$$P(E) = \sqrt{\frac{E_G}{E}} \exp\left(-\sqrt{\frac{E_G}{E}}\right). \quad (2)$$

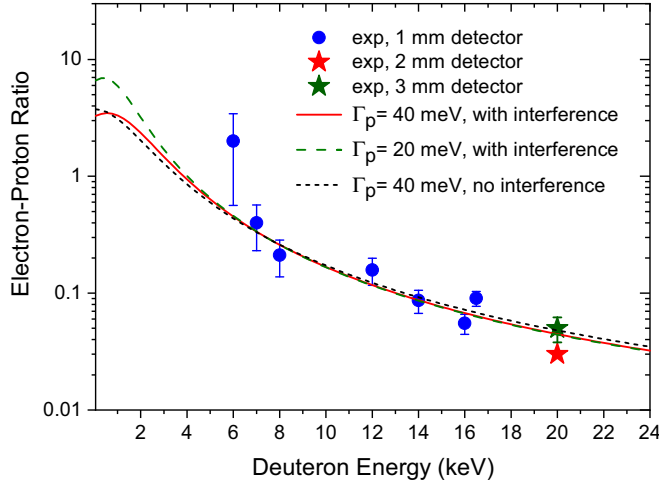


FIG. 5. Experimental electron-proton branching ratio estimated for the electron energy loss 0.6–1.0 MeV using the thin (1 mm) Si detector and compared with the theoretical calculations. The high energy point for the deuteron energy 20 keV measured with the thick (2 and 3 mm) Si detectors were renormalized to compare them to the thin detector measurements (see the text).

Here,  $E$  and  $E_G$  stand for the center-mass energy and the Gamow energy equal to  $E_G = \frac{2\pi^2}{137^2} \mu c^2$ , respectively, and  $\mu$  is the reduced mass. The screening energy  $U_e$  determines the reduction of the Coulomb barrier height. For the deuteron energy below 50 keV, the astrophysical  $S$  factor is very well known and can be presented as a linear energy function [16].

The cross section of the  $0^+$  threshold resonance can be simply expressed by the Breit-Wigner formula:

$$\sigma_{\text{res}} = \frac{\pi}{k^2} \frac{\Gamma_d \Gamma_p}{(E - E_{\text{res}})^2 + \frac{1}{4} \Gamma_{\text{tot}}^2}, \quad (3)$$

where the deuteron partial width strongly depends on energy and is given by

$$\Gamma_d(E) = 2kaP(E) \frac{\hbar^2}{\mu a^2} |\theta_d|^2, \quad (4)$$

Here  $k$  and  $a$  denote the deuteron wave number and the channel radius, respectively.  $\theta_d$  is the reduced resonance width equal to unity, assuming the single-particle resonance structure. For the deuteron energy studied, the total resonance width  $\Gamma_{\text{tot}}$  is dominated by the deuteron partial width and the other contributions can be neglected. Additionally, taking into account that both the resonance energy  $E_{\text{res}}$  and the total resonance width are much smaller than the deuteron energy, the resonance cross-section expression can be further simplified:

$$\begin{aligned} \sigma_{\text{res}} &\cong \frac{\pi}{k^2} \frac{2kaP(E+U_e) \frac{\hbar^2}{\mu a^2} \Gamma_p}{E^2} \\ &= \frac{\pi}{k} P(E+U_e) \frac{2\hbar^2}{\mu a} \frac{\Gamma_p}{E^2}. \end{aligned} \quad (5)$$

Consequently, the total cross section of the  ${}^2\text{H}(d, p){}^3\text{H}$  reaction can be presented as a sum of two contributions: the structureless “flat” component describing the known broad

and overlapping resonances in  ${}^4\text{He}$  and the component owing to the narrow threshold resonance. In the case of the incoherent sum, we get

$$\sigma_p = \frac{\pi}{k} P(E+U_e) \left[ \frac{k}{\pi} \frac{1}{\sqrt{EE_G}} S(E) + \frac{2\hbar^2}{\mu a} \frac{\Gamma_p}{E^2} \right]. \quad (6)$$

As shown previously [5], the  $0^+$  threshold resonance can, however, interfere with the known broad  $0^+$  resonances of  ${}^4\text{He}$  contributing to the excitation function  $\sigma_{\text{flat}}$ . Thus, the coherent  $0^+$  contribution to the total cross section can be expressed as follows:

$$\sigma_p^{0^+} = \sigma_{\text{flat}}^{0^+} + \sigma_{\text{res}} + 2\sqrt{\sigma_{\text{flat}}^{0^+} \sigma_{\text{res}}} \cos(\varphi_{\text{flat}}^{0^+} - \varphi_{\text{res}}), \quad (7)$$

where  $\varphi_{\text{res}}$ , the resonance phase shift given by

$$\text{tg} \varphi_{\text{res}} = \frac{\Gamma_{\text{tot}}}{2(E - E_{\text{res}})} \rightarrow 0, \quad (8)$$

takes very low values and can be neglected in Eq. (7).  $\varphi_{\text{flat}}^{0^+}$  represents the nuclear phase shift of the  $\alpha_0 = \langle {}^1S_0 | 0^+ | {}^1S_0 \rangle$  transition matrix element [17]. Therefore, in the coherent case, the proton emission cross section reads as follows:

$$\begin{aligned} \sigma_p &= \frac{\pi}{k} P(E+U_e) \left[ \frac{k}{\pi} \frac{1}{\sqrt{EE_G}} S(E) + \frac{2\hbar^2}{\mu a} \frac{\Gamma_p}{E^2} \right. \\ &\quad \left. + 2 \left( \frac{k}{\pi} \frac{S(E)}{3} \frac{1}{\sqrt{EE_G}} \frac{2\hbar^2}{\mu a} \frac{\Gamma_p}{E^2} \right)^{1/2} \cos(\varphi_{\text{flat}}^{0^+}) \right]. \end{aligned} \quad (9)$$

In the interference term of the expression above, we take into account that the  $\alpha_0 = \langle {}^1S_0 | 0^+ | {}^1S_0 \rangle$  transition makes about 1/3 of the total cross section [17].

For the electron-positron pair creation, we assume that only the threshold resonance contributes. Contribution of the known broad resonances should be much smaller due to the higher angular momenta of the corresponding transitions, and the resonance strength would be spread over a large energy range. Therefore, the corresponding cross section takes the resonant form:

$$\sigma_{\text{res}} = \frac{\pi}{k} P(E+U_e) \frac{2\hbar^2}{\mu a} \frac{\Gamma_{\text{pair}}}{E^2}. \quad (10)$$

Finally, it is clear that the resulting branching ratio between the pair creation and proton emission cross sections does not depend on the penetration factor and the screening energy anymore and can be easily fitted to the experimental data (Fig. 5).

**Results.** The experimental electron-proton ratio as measured by the 1-mm-thick detector is presented in Fig. 5. The number of electrons has been obtained by integration of counts in the energy region of spectrum, where emission of electrons/positrons dominates over other components, corresponding to the absorption bump (energy region 0.6–1.0 MeV, above the triton line, blue area in Fig. 5). According to the GEANT4 calculations, this energy region covers  $42 \pm 2\%$  of the total electron/positron number. The stopping power and ranges of positrons in Si are only about 2% lower than for electrons [18]. It means that the energy spectrum of detected positrons does not need to be considered separately and the

TABLE I. Ratio of the proton and pair creation partial resonance widths estimated for different fitting cases as described in the text.

	$\Gamma_p = 40$ meV		$\Gamma_p = 20$ meV
	Coherent	Incoherent	Coherent
$\Gamma_{\text{pair}}$ (meV)	$170 \pm 20$	$190 \pm 30$	$170 \pm 20$
$\Gamma_{\text{pair}}/\Gamma_p$	$4.3 \pm 0.5$	$4.8 \pm 0.7$	$8.6 \pm 1.0$

number of emitted electrons can be simply increased by a factor of 2. In the case of the 2- and 3-mm detectors, thicker Al foils have been used, so that we could remove from the energy spectrum not only  $^3\text{He}$  particles, but also tritons. Therefore, entire absorption bump regions could be integrated, and the corresponding fractions of electrons/positrons were  $70 \pm 4\%$  and  $80 \pm 5\%$  for the 2- and 3-mm detectors, respectively. Consequently, the experimental data obtained for both thicker detectors have been renormalized to put them together with data of the 1-mm detector in Fig. 5.

The theoretical curves were fitted to the experimental data, taking into account or neglecting the interference effect (Fig. 5). The only free fitting parameter was the partial resonance width of the internal pair creation (see Table I). The cross-section function of the proton emission was taken from Ref. [5], where the proton width was determined to be  $\Gamma_p = 40$  meV and the nuclear phase shift  $\varphi_{\text{flat}}^{0^+} = 115^\circ$ . We can see that the interference effect does not strongly influence the energy dependence of the branching ratio in the investigated deuteron energy region. Larger differences can be observed only at the lower energies. For a comparison, the theoretical curve for the proton resonance width of 20 meV is also given. Once again, the differences can be found at the lower energies. The partial resonance widths of the pair creation estimated for different cases take significantly higher values than those of the proton channel.

*Discussion and conclusions.* Indications of the electron emission have been observed in the DD reactions at very low energies. This might be attributed to the decay of the threshold resonance by means of the internal pair creation. This  $0^+$  resonance was previously observed in the  $^2\text{H}(d, p)^3\text{H}$  reaction preceding in both metallic Zr and gaseous environments [5,6]. The energy spectrum of the measured electrons/positrons agrees very well with the results of simulations performed

using the GEANT4 code. Additionally, the energy dependence of the electron-proton branching ratio determined for the deuteron energies between 6 and 16 keV can be also very well explained with excitation of the threshold resonance. For broad resonances of  $^4\text{He}$ , we would expect a constant branching ratio not exceeding the lowest measured value of about 0.03. This confirms that their small contribution could be neglected in our first analysis. The fit curves depicted in Fig. 5 describe two different models for taking into account the threshold resonance: with and without the interference effect [Eqs. (6) and (9)]. According to the fitting procedure, a constant contribution to the branching ratio should be smaller than 0.2. The differences between the theoretical curves are very small in the studied energy range. Similarly, the change of the proton partial width which was estimated in the earlier study of the  $^2\text{H}(d, p)^3\text{H}$  reaction within the experimental uncertainty does not influence the shape of the theoretical curve significantly. Likewise, the different theoretical models lead to only slightly different values of the partial pair-creation widths. The largest one equal to  $190 \pm 30$  meV was obtained for the incoherent threshold resonance amplitude. All the values are within the range predicted on the basis of the  $E0$  energy weighted sum rule [6]. To distinguish between the different resonance parameters, measurements at the deuteron energies below 5 keV will be necessary, which will be increasingly difficult due to dropping cross section. Theoretically, the  $0^+$  threshold resonance can decay by the internal electron conversion, as well. But the process is many orders of magnitude less probable than pair creation at such a high excitation energy and would result in a sharp, discrete line in the electron spectrum, which is not observed. Similarly, a decay to other excited states in  $^4\text{He}$  is strongly suppressed because of weak coupling between 2+2 and 3+1 cluster states. The suppression factor should be of order  $10^{-7}$  which corresponds to the ratio of partial resonance widths of the proton and deuteron channels observed in the  $^2\text{H}(d, p)^3\text{H}$  reaction.

Despite the experimental difficulties, this work provides a strong and independent argument for the existence of the  $0^+$  threshold resonance in the DD reactions and might have large consequences for the nuclear astrophysics and the nuclear fusion applied studies.

*Acknowledgments.* This project received funding from the European Union's Horizon 2020 research and innovation program under Grant Agreement No. 951974.

- 
- [1] D. R. Tilley, H. R. Weller, and G. M. Hale, *Nucl. Phys. A* **541**, 1 (1992).  
 [2] H. M. Hofmann and G. M. Hale, *Phys. Rev. C* **77**, 044002 (2008).  
 [3] K. Arai, S. Aoyama, Y. Suzuki, P. Descouvemont, and D. Baye, *Phys. Rev. Lett.* **107**, 132502 (2011).  
 [4] S. Aoyama *et al.*, *Few-Body Syst.* **52**, 97 (2012).  
 [5] K. Czerski *et al.*, *Europhys. Lett.* **113**, 22001 (2016).  
 [6] K. Czerski, *Phys. Rev. C* **106**, L011601 (2022).  
 [7] E. Hiyama, B. F. Gibson, and M. Kamimura, *Phys. Rev. C* **70**, 031001(R) (2004).  
 [8] E. E. Salpeter, *Aust. J. Phys.* **7**, 373 (1954).  
 [9] S. Ichimaru and H. Kitamura, *Phys. Plasmas* **6**, 2649 (1999).  
 [10] A. Huke, K. Czerski, P. Heide, G. Ruprecht, N. Targosz, and W. Zebrowski, *Phys. Rev. C* **78**, 015803 (2008).  
 [11] C. Spitaleri *et al.*, *Phys. Lett. B* **755**, 275 (2016).

- [12] S. Agostinelli *et al.*, *Nucl. Instrum. Methods Phys. Res. A* **506**, 250 (2003).
- [13] K. Kaczmarek *et al.*, *Acta Phys. Pol. B* **45**, 509 (2014).
- [14] G. Das Haridas, R. Dubey, K. Czerski, M. Kaczmarek, A. Kowalska, N. Targosz-Sieczka, and M. Valat, [arXiv:2312.12446](https://arxiv.org/abs/2312.12446).
- [15] K. Czerski *et al.*, *Europhys. Lett.* **68**, 363 (2004).
- [16] R. E. Brown and N. Jarmie, *Phys. Rev. C* **41**, 1391 (1990).
- [17] H. Paetz gen. Schieck, *Eur. Phys. J. A* **44**, 321 (2010).
- [18] M. J. Berger and S. M. Seltzer, Report No. NBSIR 82-2550 (1982).